Pharmaceutical Research, Vol. 22, No. 11, November 2005 (© 2005)
DOI: 10.1007/s11095-005-7248-2

Research Paper

Membrane Binding Proteins are the Major Determinants for the Hepatocellular Transmembrane Flux of Long-Chain Fatty Acids Bound to Albumin

G. Rajaraman,[1] M. S. Roberts,[2] D. Hung,[2] G. Q. Wang,[1] and F. J. Burczynski[1,3,4]

Received December 23, 2004; accepted July 6, 2005

Purpose. The hepatic transmembrane flux of long-chain fatty acids (LCFA) occurs through passive and fatty acid transport protein facilitated processes from blood. The extent that these transport processes can be related to the unbound and protein-bound fractions of LCFA in blood is not clear.
Methods. We used hepatocyte suspensions, hepatoma monolayers, and perfused rat livers to quantitate the transport of purified [^{3}H]palmitate ([^{3}H]PA) and 12-(*N*-methyl)-*N*-[(7-nitrobenz-2oxa-1,3-diazol-4yl-)amino]octadecanoicacid (12-NBDS) from solutions with a constant unbound LCFA concentration with varying bovine serum albumin (BSA) concentrations and in the presence and absence of antisera raised against cytosolic liver fatty acid binding protein (L-FABP).
Results. In the absence of L-FABP antisera, using an unbound ligand concentration that was adjusted to remain constant at each BSA concentration, hepatocyte [^{3}H]PA and 12-NBDS uptake rates increased linearly with an increase in BSA concentration ($p < 0.0001$). In the presence of L-FABP antisera, [^{3}H]PA uptake showed a greater reduction in the presence of 100 μM BSA than 5 μM BSA. The calculated permeability surface area product (PS) confirmed that both unbound and bound fractions of LCFA contributed to the overall flux, but only the PS for the protein-bound fraction was reduced in the presence of L-FABP antisera. *In situ* rat liver perfusion studies showed that the only rate process for the disposition of [^{3}H]PA in the liver inhibited by L-FABP antisera was that for influx, as defined by PS, and that it reduced PS in the perfused liver by 42%.
Conclusion. These results suggest that, at physiological albumin concentrations, most of the LCFA uptake is mediated from that bound to albumin by a hepatocyte basolateral membrane transport protein, and uptake of unbound LCFA occurring by passive diffusion contributes a minor component.

KEY WORDS: albumin; FABP; hepatocyte; liver; long-chain fatty acid; palmitate; stearate; uptake.

INTRODUCTION

Long-chain fatty acids (LCFA) are highly lipophilic protein-bound substrates utilized by cells to meet energy demands and synthesize cellular components. Understanding the fundamentals of the uptake process for these hydrophobic organic anions is both crucial and central in mapping their intracellular disposition. This is of paramount importance in clinical disorders such as nonalcoholic steatohepatitis, cholestasis, etc. Although these substrates are extensively albumin-bound, hepatocytes extract them with a very high efficiency (1,2). The presence of sinusoidal fenestrations together with the lobular architecture of the liver help provide a large surface area for the albumin-bound complexes to interact. Although there is a vast body of literature available regarding the cellular transmembrane flux of these ligands, still unclear are events occurring at the outer plasma membrane leaflet, specifically, with respect to the role of extracellular binding proteins in the uptake process (3–7).

According to conventional theory for the cellular uptake of highly protein bound ligands, only unbound ligand participates in the uptake process. The protein bound fraction serves only to replenish the amount of substrate depleted by the uptake process. This theory was first challenged in the mid 1960s, and since then a plethora of reports showed results to be inconsistent with the conventional model and favored some form of facilitated dissociation of protein-bound ligands (8–14). An important recent realization is the role of the fatty acid binding protein (FABP) as a facilitator of LCFA transport both across the cell membrane and in the cytoplasm (15,16). Because hepatocyte albumin extraction is negligible (9,17,18), the

[1] Faculty of Pharmacy, University of Manitoba, Winnipeg, Manitoba, Canada.
[2] Faculty of Pharmacy and Department of Medicine, Princess Alexandra Hospital, University of Queensland, Woolloongabba, Queensland 4102, Australia.
[3] Department of Pharmacology and Therapeutics, Faculty of Medicine, University of Manitoba, Winnipeg, Manitoba, Canada.
[4] To whom correspondence should be addressed.(e-mail: burczyn@cc.umanitoba.ca).

ABBREVIATIONS: BSA, bovine serum albumin; FABP, fatty acid binding protein; $FABP_{pm}$, Plasma Membrane Fatty Acid Binding Protein; fmol, femtomoles; [^{3}H]PA, radioactive (tritiated) palmitate; LCFA, long-chain fatty acids; L-FABP, liver fatty acid binding protein; MR, molar ratio; nmol, nanomoles; 12-NBDS, 12-(N-methyl)-N-[(7-nitrobenz-2oxa-1,3-diazol-4yl-)amino]octadecanoicacid; PA, palmitate; pmol, picomoles; PS, permeability surface area product.

most feasible model for transport seems to be that described by Stremmel's group (16). They suggested that LCFAs are presented to hepatocytes as fatty acid–albumin complexes. In the close proximity of hepatocellular membrane proteins, which have a high affinity for fatty acids, e.g., fatty acid transport protein (FATP) or the membrane 40-kDa fatty acid-binding protein ($FABP_{pm}$), these complexes dissociate and the LCFA bind to the membrane proteins as the first part of the transmembrane process. The fatty acids now flip-flop across the phospholipid membrane bilayer as uncharged ligands via a transmembrane concentration gradient and then associate with the 14-kDa cytosolic FABP (L-FABP) or with caveolin-1 at the cytosolic surface of the plasma membrane. Support for docking of fatty acid–albumin complexes with $FABP_{pm}$ rather than a prior dissociation in the vicinity of $FABP_{pm}$ is provided by Burczynski *et al.* (11). Using chemically modified albumin to yield proteins with isoelectric points (p*I*) ranging from 4.9 to 8.6 and similar dissociation rates, they reported that uptake of [^{3}H]palmitate ([^{3}H]PA) was statistically greater in the presence of proteins possessing higher p*I* values and therefore concluded that the protein–ligand complex does in fact interact with the cell's plasma membrane.

Luxon (19) used laser photobleaching in male and female livers and a L-FABP inhibitor to show that L-FABP modulates the cytoplasmic transport of NBD-stearate by reducing its binding to immobile cytosolic membranes. This mechanism was confirmed in clofibrate-induced L-FABP livers (20,21), in livers of pregnant women (22), and in diseased livers (23). Hung *et al.* (22) showed that the permeability surface area product (PS) for palmitate (PA) uptake in perfused livers for pregnant female rats was greatest followed by clofibrate-treated male rats, which was greater than in females and least in male rats, emphasizing the role played by binding proteins in PA uptake by hepatocytes.

In the present paper we investigated the hypothesis that the extent of differences in uptake from the unbound and albumin-bound fractions could be directly related to their transport by passive diffusion and membrane fatty acid binding protein facilitated transport. The relative contribution of unbound and albumin-bound PA on PA uptake rate in hepatocyte cultures was determined by varying albumin concentrations while keeping the unbound PA concentration constant. The relative importance of passive diffusion of unbound PA and membrane facilitated transport pathways were then assessed by uptake studies in the presence of rabbit antisera raised against liver fatty acid binding protein (L-FABP) in 1548 cells and by examining the extent to which the PS products had been affected. These findings were validated using perfused rat livers. To eliminate the possibility that radiolabeled impurities lead to misleading results, we repeated the studies using a fluorescent labeled LCFA (12-NBDS) in 1548-hepatoma cell monolayers.

MATERIALS AND METHODS

[^{3}H]PA (56.5 Ci/mmol) and Na[^{125}I] were purchased from New England Nuclear (Boston, MA, USA). 12-(*N*-Methyl)-*N*-[(7-nitrobenz-2oxa-1,3-diazol-4yl-)amino]octadecanoicacid (12-NBDS) was obtained from Molecular Probes (Eugene, OR, USA). Heptane was purchased from Fisher Scientific (Pittsburgh, PA, USA). All other chemicals including albumin [essentially fatty acid-free bovine serum albumin (BSA)], fetal bovine serum (FBS), palmitic acid, and stearic acid were obtained from Sigma (St. Louis, MO, USA). The aqueous buffer used throughout all experiments was phosphate-buffered saline (PBS), which had a composition of (in mM): 137 NaCl, 2.68 KCl, 1.65 KH_2PO_4, and 8.92 Na_2HPO_4. The pH was adjusted to 7.4 using 0.1 N NaOH.

Preparation of [^{125}I]BSA

To substantiate previous work showing that uptake of the BSA–ligand complex is negligible during the study period, [^{125}I]BSA uptake studies were conducted. BSA was radioiodinated by slightly modifying the chloramine-T method previously described by Greenwood and Hunter (11,24). Briefly, Na [^{125}I] (~1 mCi) and 5 mg/ml of freshly prepared chloramine-T solution were added to the prepared BSA solution in an injection vial. The contents were well mixed and allowed to react for 5 min at room temperature, after which 5 mg/ml of freshly prepared sodium metabisulfite solution was added. The contents were transferred to a molecular sieve column for separation of the iodinated BSA and free Na[^{125}I]. The [^{125}I]BSA solution was further purified by extensively dialyzing against PBS using 3,500 MWCO Spectra/Por membrane (Spectrum Labs Inc., Rancho Dominguez, CA, USA) and finally concentrated using Biomax Ultrafree Centrifugal Filters (MWCO 5,000; Millipore Corp., Bedford, MA, USA).

Purification of [^{3}H]PA

The importance of purifying radiolabeled LCFA has been previously discussed (25). In that report the authors concluded that results may be misleading without purification. Thus, we routinely purify the manufacturer-supplied [^{3}H]PA (referred to as stock [^{3}H]PA) prior to use, as previously described (25,26). Briefly, 1.0 ml of the stock [^{3}H]PA was added to 0.98 ml of distilled water (18 MΩ cm) containing 0.1 M NaOH and approximately 1 mg thymol blue. The solution was vortex-mixed with 1.2 ml of heptane for 60 s and allowed to separate into two phases. After separation, the heptane phase was discarded, fresh heptane added, and the procedure repeated another two more times. During the third extraction the aqueous phase was acidified using two drops of 6 N HCl and the mixture vortexed for 60 s. The purified [^{3}H]PA in the heptane phase was harvested, fresh heptane added to the acidified aqueous phase, and the procedure repeated twice. All of the heptane phase fractions were collected and pooled. The heptane evaporated until approximately 10–20 μl heptane remained. At this time, 1 ml of 100% ethanol was added. The purified [^{3}H]PA was stored in ethanol at −20°C until used.

Determination of Unbound PA Concentration

To examine the driving force for uptake, it is critical to keep free (unbound) ligand concentration constant at all protein concentrations being studied. The unbound [^{3}H]PA

concentration was determined by using the heptane/buffer partition ratio previously assessed for this type of analysis (25,27). Purified [^{3}H]PA (tracer concentration, ~1 nM) was added to solutions of PBS containing 5, 25, 50, 125, 250, 375, or 500 μM BSA that were freshly prepared prior to each experiment. The unbound PA concentration was measured by heptane/buffer partitioning as previously described (25,28). The unbound PA concentration was adjusted to remain constant at each BSA concentration by the addition of unlabeled PA. The unbound [^{3}H]PA fraction (α) was calculated using

$$\alpha = PR^+/PR^-$$

where PR^+ is the heptane/buffer partition ratio of [^{3}H]PA in the presence of BSA and PR^- is the heptane/buffer partition ratio in the absence of BSA. The partition ratio PR was calculated as

$$PR = TR_h/TR_b$$

where TR_h is the total radioactivity in the heptane phase and TR_b is the total radioactivity measured in the buffer phase. PR^- was not assessed in this study but the value of 702 was taken from our previous report (25). Data were obtained from six separate experiments of triplicates. Samples of both the heptane and buffer phases containing various concentrations of BSA were obtained after 24 h incubation. This time frame was sufficient for equilibrium to be achieved (27). Calculation of PA/BSA molar ratio included both the unlabeled and labeled PA.

Preparation of Hepatocyte Suspensions

Studies were performed in accordance with the principles and guidelines of the Canadian Council on Animal Care and the University of Manitoba Animal Care Committee. Female Sprague–Dawley rats (200–250 g), purchased from University of Manitoba breeding stock, were housed in a temperature- and light-controlled room (22°C; lights set on a 12-h on/off cycle starting at 0600 hours) and allowed Agway Prolab Animal Diet (Agway County Foods, Syracuse, NY, USA) and water *ad libitum*. Hepatocyte suspensions were prepared by collagenase perfusion, as we have previously described (29). Briefly, animals were anesthetized with an intraperitoneal injection of pentobarbital (50 mg/kg). An abdominal midline incision exposed the portal vein, which was cannulated. Livers were perfused *in situ* at 20 ml/min initially with oxygenated Swim's S-77 medium containing 5 mM EDTA for approximately 8 min, and thereafter with Swim's S-77 medium containing 25 mg/dL collagenase and 5 mM $CaCl_2$ for approximately 10 min. Perfused livers were excised, combed free of connective tissue, and filtered through 150-mesh followed by 50-mesh stainless steel filters (Sigma). Parenchymal cells were separated from nonparenchymal cells by centrifugation at 55 *g* for 3 min. The isolated hepatocytes, which represented more than 95% of the isolated cell population, were stored at room temperature and used within 2 h. Cell viability was greater than 90%, as assessed microscopically by visualizing cells using Trypan blue exclusion criteria before and after uptake experiments.

Hepatocyte [^{3}H]PA and [^{125}I]BSA Uptake

We used the rapid filtration technique, a well-validated method for studying ligand uptake by isolated hepatocyte suspensions, to study hepatocyte PA uptake (30–32). Hepatocytes were added to BSA solutions (37°C), which also contained labeled (either purified or stock [^{3}H]PA, ~1 nM) and unlabeled PA. Uptake experiments using purified [^{3}H]PA were performed at a constant unbound PA concentration (using PA/BSA molar ratios from Fig. 2), whereas experiments using unpurified or stock [^{3}H]PA were performed at a fixed PA/BSA molar ratio of 0.3:1. Hepatocytes (~3.4×10^5 hepatocytes/ml) were prevented from sedimentation by gently agitating the incubating solution. At 30-s intervals, 0.8-ml aliquots of the cell suspension were immediately vacuum-filtered through Whatman GF/C membranes and washed with 7 ml of ice-cold PBS to stop uptake and wash any extracellular radiolabeled ligand. The final wash step has been shown to prevent the transmembrane flux of [^{3}H]PA and to remove any adhering [^{3}H]PA containing solution (33). Radioactivity was quantitated using a Beckman LS6500TA liquid scintillation counter. The same procedure was adopted for determining hepatocyte [^{125}I]BSA uptake. Radioactivity measurements in this case were performed on a LKB 1272 clinigamma counter. Uptake was calculated using least squares regression analysis of the plot of amount of cellular PA *vs.* time.

Cell Culture

Rat hepatoma cells (1548 cell line) were maintained in Dulbecco's modified Eagles medium (DMEM), 10% FBS, penicillin (100 U/mL), and streptomycin (100 μg/mL) at 37°C in a humidified atmosphere of 5% CO_2.

12-NBD Stearate Uptake

It could be argued that uptake results using [^{3}H]PA also reflect uptake by radiolabeled impurities that may be still present in our solution despite our efforts to minimize those errors. Thus, LCFA uptake by 1548 rat hepatoma monolayer cultures was studied using the fluorescent 12-NBD stearate analog. Storch *et al.* (34) described a quantitative fluorescence method for studying the uptake of the fluorescent fatty acid analog (*n*-AOFFA) by adipocytes. We adapted this method for studying the uptake of LCFA by hepatocyte monolayers. Total stearate uptake was expressed in fluorescence units. A Nikon inverted microscope, with epifluorescence optics, was used to record the fluorescence intensity over time of the fluorescent probe 12-NBD stearate (488-nm excitation wavelength and 530-nm emission wavelength). The method used was modified from previously described procedures (34,35). Uptake studies used the cultured 1548 hepatoma cells grown in monolayer on 24-well plates. One hour prior to uptake measurements, cells were incubated with fresh serum-free media. A 200-μL aliquot of various BSA solutions (5–500 μM) containing fluorescent 12-NBDS (adjusted molar ratio to obtain the same unbound ligand concentration from [^{3}H]PA data) was added to each well. At specified time points (30-s intervals), the solution was

quickly aspirated and cells washed twice with ice-cold PBS (to wash off any extracellular probe). Images were acquired in the frame mode using 488-nm argon laser and emission light recorded after passing a 515- to 565-nm band pass filter. The recorded images were later analyzed using an Axon Integrated Imaging System (Axon Instruments, Foster City, CA, USA). The increase in fluorescence intensity over time was taken to reflect hepatocyte 12-NBDS uptake. The initial increase in cellular fluorescence (12-NBDS influx) at each BSA concentration was studied at 30-s intervals.

Preparation of FABP Antisera

Antisera was raised against rat liver cytosolic fatty acid binding protein (L-FABP) by an intradermal injection of the purified antigen in Freund's complete adjuvant into female New Zealand White rabbits, followed by biweekly intramuscular booster injections of the antigen (22,36). Rabbit plasma was harvested and stored frozen (−20°C) until required.

[^{3}H]PA Clearance by 1548 Hepatoma Cells in Presence of Antisera

To ensure that the 1548 hepatoma cells have similar LCFA uptake properties to hepatocytes isolated from healthy rats, we conducted clearance studies using purified [^{3}H]PA in the presence of 100 and 5 μM BSA and calculated the clearance ratio rates at these two BSA concentrations. The purified [^{3}H]PA monolayer uptake study was performed as previously described (18). The 1548 hepatoma cells grown in culture flasks were subcultured and seeded onto 24-well plates in DMEM containing 10% FBS. After 24 h of incubation, cells were further incubated for 4 h in the presence of serum-free DMEM. Prior to uptake, cells were incubated with 1:50 (vol/vol) L-FABP antisera (1:50 rabbit serum in control experiments) in serum-free DMEM for 30 min, after which the media was quickly aspirated, washed twice with 37°C PBS, and incubated with BSA solution (5 and 100 μM) containing purified [^{3}H]PA radiolabel (1 nM). At 30-s intervals, the incubation solution was quickly aspirated, washed once with ice cold PBS, and cells were incubated with lysis buffer (1% Triton buffer) for a further 15 min. The cell lysate was counted for radioactivity using Beckman LS6500TA liquid scintillation counter.

In Situ Rat Liver Perfusions

In situ studies were performed in accordance with the University of Queensland Animal Care Committee guidelines. Male Wistar rats (300–350 g body weight), purchased from The University of Queensland Central breeding stock, were housed in a temperature- and light-controlled room (22°C; lights set on a 12-h on/off cycle starting at 0600 hours) and allowed Rat & Mouse Nuts (Norco Stockfeeds, South Lismore, NSW, Australia) and water *ad libitum*. The night prior to surgery animals were fasted. The surgical procedure used in this study has been described previously (22,23,37). Briefly, rats were anesthetized by an interperitoneal injection of 10 mg/kg xylazine (Bayer, Sydney, Australia) and 80 mg/kg ketamine hydrochloride (Parnell Laboratories, Sydney, Australia). Following laparotomy animals were heparinized (heparin sodium, 200 units; David Bull Laboratories, Mulgrave, Australia) via the inferior vena cava. The bile duct was cannulated with PE10 (Clay Adams, Parsippany, NJ). The portal vein was cannulated using a 16-gauge i.v. catheter and the liver perfused via this cannula with 1% fatty acid-free BSA dissolved in PBS. Prior to entry into the liver, the perfusate was oxygenated using a silastic tubing lung ventilated with 100% oxygen. The perfusion system used was a nonrecirculating and employed a peristaltic pump (Cole-Parmer Instrument, Vernon Hills, IL, USA). Following the initiation of liver perfusion, animals were sacrificed by thoracotomy and the thoracic inferior vena cava was cannulated using PE 240 (Clay Adams). Oxygen consumption, bile flow, perfusion pressure, and macroscopic appearance were checked to assess liver viability.

Bolus Studies

Each liver was perfused at a rate of 25 mL/min. After a 10-min perfusion stabilization period, a 50-μL injection of [^{14}C]sucrose (1.5×10^6 dpm) and purified [^{3}H]PA (3×10^6 dpm) (Bolus 1) was administered through the portal vein cannula. Bolus injections were completed in less than 1 s. Prior to introduction of the Hamilton syringe injection needle into the flowing perfusate, the injection needle barrel was wiped with a tissue wetted with heptane to remove any adhered [^{3}H]PA on the outside of the stainless steel needle. Experiments in which the needle barrel was not wiped with heptane were associated with slightly higher initial outflow profiles, i.e., the first three outflow data points were significantly higher than the [^{14}C]sucrose data points. Thus, the heptane wipe procedure eliminated any error associated in the outflow samples during the initial upslope phase of the outflow concentration–time curves due to adhered [^{3}H]PA. Outflow samples were collected using a fraction collector over 90 s (1 s × 20, 4 s × 5, 10 s × 5). Following the first bolus injection, a second bolus injection was administered in a similar manner with outlet samples being collected at identical time intervals. Composition of the second bolus injection contained [^{3}H]water (3×10^6 dpm). Aliquots (100 μL) of effluent samples from the first bolus injection were counted for [^{14}C]sucrose radioactivity and total tritiated radioactivity ([^{3}H]PA and any [^{3}H]metabolites that may be present) using a MINAXI beta TRI-CARB 4000 series liquid scintillation counter (Packard Instruments, Meriden, CT, USA). Effluent samples from the second bolus dose ([^{3}H]water) were analyzed in an identical manner.

A modification of the Dole procedure (38) was used to separate [^{3}H]PA from any [^{3}H]fatty acid metabolites (22). Briefly, an aliquot (100 μL) of effluent sample (contained in a 2-mL Eppendorf tube) containing 1% BSA was treated with 50 μL of 10% TCA. Following precipitation, samples were centrifuged for 4 min at 13,000 rpm and the supernatant was discarded. The Eppendorf tube containing the pellet was cut at the level just above the pellet and placed directly into a scintillation vial containing 2 ml Ready Safe scintillate. The pellet was allowed to dissolve overnight and BSA-associated radioactivity (representing [^{3}H]PA) was determined the following day. Two interventions, consisting of two bolus injections of radiolabeled material, were performed in each

perfused liver. Livers were initially perfused with perfusate containing 1% BSA followed by perfusion with 1% BSA and rabbit plasma containing L-FABP antisera. The vol/vol ratio of perfusate/rabbit plasma was 700:1.

Data Analysis

The outflow concentrations for solutes were presented as outflow fraction per milliliter. The resulting outflow concentration–time profiles were then analyzed using the two-phase extended convection–dispersion model. A detailed description of the theory and method for modeling is reported elsewhere (39). Briefly, the concentration–time profile for the vascular marker sucrose was modeled by the following equation in Laplace domain:

$$\hat{C}_s(s) = \frac{1}{Q}\exp\left(-st_{lag} + \frac{1-\sqrt{1+4D_N T_s(s+a-ab/(s+b))}}{2D_N}\right) \quad (1)$$

where Q is the flow rate, D_N is the dispersion number, T_s is the time parameter for sucrose, t_{lag} is the lag time due to the catheter and large nonexchanging vessels, and a and b are the rate parameters to correctly describe the tail section of the concentration–time profile. The mean transit time for sucrose can then be determined as:

$$MTT_s = T_s\left(1+\frac{a}{b}\right) \quad (2)$$

The PA concentration time profile has been modeled as:

$$\hat{C}_p(s) = \frac{1}{Q}\exp\left(-st_{lag} + \frac{1-\sqrt{1+4D_N T_s\beta(f(s)+a-ab/(f(s)+b))}}{2D_N}\right) \quad (3)$$

where parameter β describes the difference in extracellular space volume between the sucrose and PA, and $f(s)$ describes the cellular behavior of the drug. For the two-phase model, we have:

$$f(s) = s + k_1 - \frac{k_1 k_2}{s + k_e + k_2} \quad (4)$$

where k_1 is the permeation rate constant ($=PSfu_P/V_P$, PS is the permeability-surface product, fu_P is the free fraction of the solute in the perfusate, and V_P is the volume of distribution of PA in the perfusate), k_2 is the efflux rate constant, and $k_e = Cl_{\text{int}}/V_C$ is the intrinsic elimination clearance normalized per hepatocellular volume, V_C.

When diffusion in hepatocytes is a rate-limiting function, equation for $f(s)$ becomes:

$$f(s) = s + k_1 - \frac{k_1 k_2}{\sqrt{k_d(s+k_e)}\tanh\left(\sqrt{(s+k_e)/k_d}\right) + k_2} \quad (5)$$

where k_d is the diffusion rate constant ($=D/h^2$, D is the coefficient of diffusion in hepatocytes and h is the effective thickness of the hepatocytes).

The fractional outflow-*vs.*-time data were fitted in the time domain by using a numerical inverse Laplace transformation of the appropriate transit time density function applying the nonlinear regression program SCIENTIST (MicroMath Scientific Software, Salt Lake City, UT, USA). Data were analyzed by a sequential procedure; first, the fractional outflow curve $C_s(t)$ of the extracellular marker [^{14}C]sucrose was fitted using Eq. (1). Parameters T_s, D_N, and t_{lag} were determined first (whereas a was set to zero) by fitting with the equal weighting, then these parameters were fixed, and a and b were determined by fitting with weighting of $1/y_{\text{observed}}$. Parameters for sucrose were then fixed, and k_1 and β were determined (whereas k_2 was set to zero) by fitting the concentration–time profile for [^{3}H]PA with the equal weighting using Eq. (3), with $f(s)$ determined in Eqs. (4) or (5). Parameter β was then fixed, and k_1, k_2, k_e, and k_d were determined by fitting PA data with weighting of $1/y_{\text{observed}}$. It was found that the diffusion rate constant (k_d) was increased to infinity while fitting the PA data. It was therefore concluded that diffusion in hepatocytes was not rate limiting, and the two-phase model [Eq. (3) with $f(s)$ determined in Eq. (4)] is concluded to represent PA data.

Nonparametric estimates of hepatic availability (F) of [^{3}H]PA in various models were determined from the outflow concentration (C)-*vs.*-time (t) profiles from Eq. (6) using the parabolas-through-the-origin method (extrapolated to infinity) with the assistance of the Moments Calculator 2.2 program for Macintosh computer (Purves, 1992).

$$F = \frac{Q \bullet AUC}{D} \quad (6)$$

where AUC = $\int_0^\infty C(t)dt$ is the area under the solute concentration-*vs.*-time curve, Q is the perfusate flow rate, and D is the dose of solute administered. All concentrations used were expressed in molar equivalents. Hepatic extraction ratio (E) equals to $1 - F$.

$$MTT = \frac{AUMC}{AUC} \quad (7)$$

AUMC is the area under the first moment curve.

$$CV^2 = \frac{\sigma^2}{MTT^2} \quad (8)$$

where

$$\sigma^2 = \frac{\int_0^\infty t^2 C(t)dt}{\int_0^\infty C(t)dt} - MTT^2 \quad (9)$$

Permeability Surface Area Product (PS) Calculation

Uptake of purified [^{3}H]PA comes from two components: transport and diffusion. Previous work has shown that both the BSA–PA and the unbound PA fractions are involved in the uptake process (4,12,13). Accordingly, we modeled the PS product for transport and diffusion using total [^{3}H]PA uptake data from isolated hepatocytes and 1548 hepatoma

cells [^{3}H]PA uptake experiments (the latter performed both in the presence and absence of antisera) according to:

$$J_x = PS_T C_{Tx} + PS_U C_{Ux} \quad (10)$$

$$J_y = PS_T C_{Ty} + PS_U C_{Uy} \quad (11)$$

where J is the flux of [^{3}H]PA into the cell (mol/s or mol/10^6 cells/s); PS_T and PS_U are the permeability surface area products (transport and diffusion, respectively; L/s or L/10^6 cells/s); C is the ligand concentration (mol/L); and the subscripts, T, U, x, and y denote total ligand concentration and unbound ligand concentration at two different BSA concentrations (where x was fixed at 5 μM and y denoted a BSA concentrations >5 μM). Equations (10) and (11) were solved for PS_T and PS_U by comparing 5 μM BSA with all BSA concentrations. In the case of isolated hepatocyte PA uptake experiments, the products $PS_T{*}C_{Tx}$ and $PS_U{*}C_{Ux}$, which represent the transport and diffusive components of total PA uptake, respectively, were plotted against increasing BSA concentrations. We made the assumption that only unbound or free PA diffuses across the plasma membrane, whereas both the unbound and protein-bound ligands interact with the transport component(s) of the plasma membrane and that the parameters PS_U and PS_T are BSA-independent. For the 1548 hepatoma PA clearance studies, total PA uptake was calculated by using a total PA concentration of 1 nM (tracer [^{3}H]PA). The resultant flux for 100 μM BSA was then resolved into transport ($PS_T{*}C_{T100}$) and diffusive ($PS_U{*}C_{U100}$) components, using Eqs. (10) and (11) both in the presence and absence of L-FABP antisera.

Statistical Analyses

Data are presented as mean ± SEM unless otherwise stated. The n value refers to the number of animals (in the case of isolated hepatocytes or *in situ* rat liver perfusions) or number of plates (in the case of hepatoma cells) or number of replicates performed for each study. Data were analyzed using linear regression analysis and Student's t tests. The minimum level for statistical significance was set at $p < 0.05$.

RESULTS

Defining Unbound and Protein bound [^{3}H]PA Concentration. Figure 1 shows the various unbound PA concentrations obtained over a range of BSA concentrations (μM) for PA/BSA molar ratios of 0.1:1 to 2:1. It is evident that a constant unbound PA concentration is most readily achieved with the lowest molar ratio and that, at higher ratios, the unbound PA concentration increased with an increase in the PA/BSA molar ratio. Figure 1 also shows that stock [^{3}H]PA gives a higher unbound PA concentration than an equivalent purified PA, consistent with radiolabeled impurities leading to an overestimation of unbound PA concentration when nonpurified [^{3}H]PA is used. Figure 2 shows the observed unbound PA concentrations obtained when PA/BSA molar ratios were adjusted with cold (unlabeled) PA and purified [^{3}H]PA for different BSA concentrations with a goal of achieving a constant unbound PA concentration of 2 nM. The resulting unbound PA concentration was not significantly different over the range of BSA concentrations ($p > 0.05$). The addition of unlabeled PA statistically reduced the PA/BSA molar ratio from the unadjusted values shown in Fig. 1.

Uptake of [^{3}H]PA by Isolated Rat Hepatocytes. Hepatocyte uptake of purified [^{3}H]PA at the different BSA concentrations is shown in Fig. 3. A linear relationship was evident for purified PA, whereas a curvilinear relationship was evident for stock (impure PA). The linear regression line had a slope of 0.011 ± 0.001 pmol/s/μM BSA/10^6 cells ($n = 6$), a correlation coefficient (r) of 0.97, and was significantly different from zero ($p < 0.0001$). In contrast, an apparent saturation of PA uptake by isolated hepatocytes at a fixed PA/BSA molar ratio of 0.3:1 is evident at a concentration of about 100 μM BSA using stock solutions of PA.

Hepatocyte Uptake of [^{125}I]BSA. No substantial hepatocyte uptake of labeled [^{125}I]BSA ($p > 0.05$) ($n = 6$), using the same PA/BSA molar ratios as in the [^{3}H]PA uptake studies, was evident. The slope of the [^{125}I]BSA clearance was not statistically different from zero, −0.0027 ± 0.0368 nL/s/μM/10^6 cells with a correlation coefficient of 0.01. Thus, we conclude that there was no substantial uptake of the PA–BSA complexes by hepatocytes during the time interval used in this study and that the LCFA was being transported across the hepatocyte membrane in a nonprotein-bound form.

1548 Hepatoma Uptake of 12-NBDS. The clearance ratio of 5 μM (Cl_5) to 100 μM BSA (Cl_{100}) by isolated rat hepatocytes was not statistically different from the clearance ratio calculated using the 1548 hepatoma cell line (Cl_5/Cl_{100} = 3.2 ± 0.2 and Cl_5/Cl_{100} = 3.0 ± 0.1, respectively, $n = 6$). Thus, we concluded the 1548 hepatoma cell line reflected similar LCFA uptake properties to those of isolated hepatocytes allowing us to use 1548 hepatoma cells for 12-NBDS studies. Figure 4 shows 12-NBDS uptake (arbitrary fluorescence units) *vs.* BSA concentration ($n = 5$). Although 12-NBDS

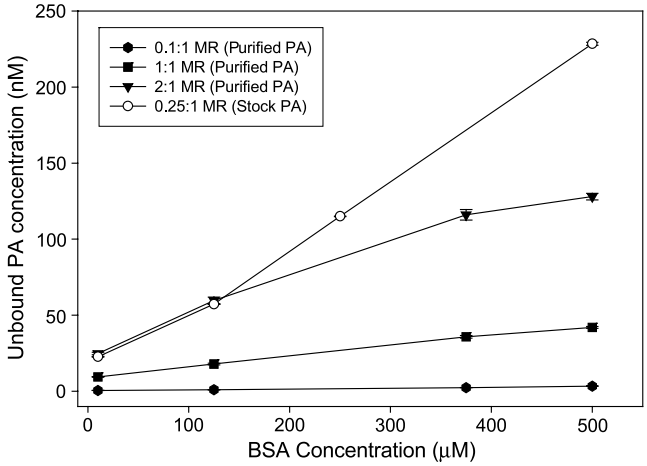

Fig. 1. Plot of unbound palmitate (PA) concentration (nM) determined using purified [^{3}H]PA and stock [^{3}H]PA (manufacturer-supplied unpurified [^{3}H]PA) *vs.* BSA concentration (range 10–500 μM) at various PA/BSA molar ratios (MR). Unbound PA concentrations were determined by heptane/buffer partitioning at 37°C for 24 h. Each data point represents the mean ± SEM ($n = 6$).

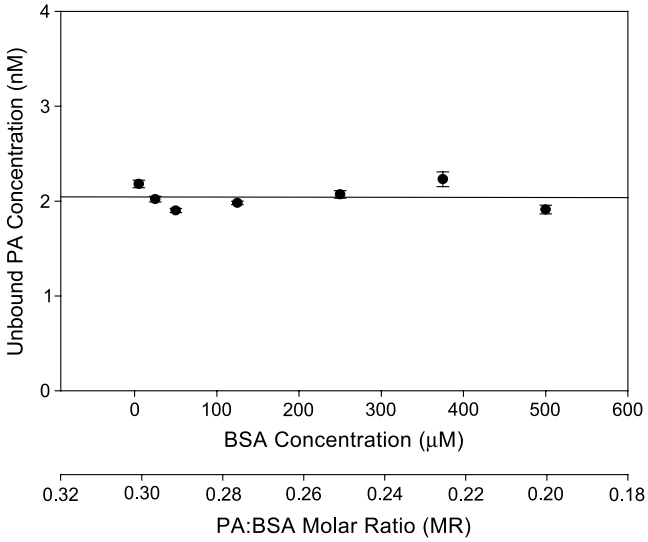

Fig. 2. Plot unbound PA concentration (nM) at different BSA concentrations (5–500 μM). Various amounts of unlabeled PA were added to adjust PA/BSA molar ratio (MR) in order for the unbound PA concentration to remain constant. Total palmitate added was 100, 93.7, 62.5, 31.2, 14.0, 7.5, and 1.5 μM at BSA concentrations of 500 μM (0.2 MR), 375 μM (0.25 MR), 200 μM (0.25 MR), 125 μM (0.25 MR), 50 μM (0.28 MR), 25 μM (0.3 MR), and 5 μM (0.3 MR), respectively. The adjusted MR was found to be a decreasing function of BSA concentration when constant unbound PA was attained. Unbound PA concentration at the different BSA concentration was not statistically different. Data represent mean ± SEM (n = 6).

uptake qualitatively seemed to be linearly related to BSA over the range of BSA concentrations studied (correlation coefficient of 0.97), it may also be possible to describe the data by a curvilinear relationship with saturation kinetics

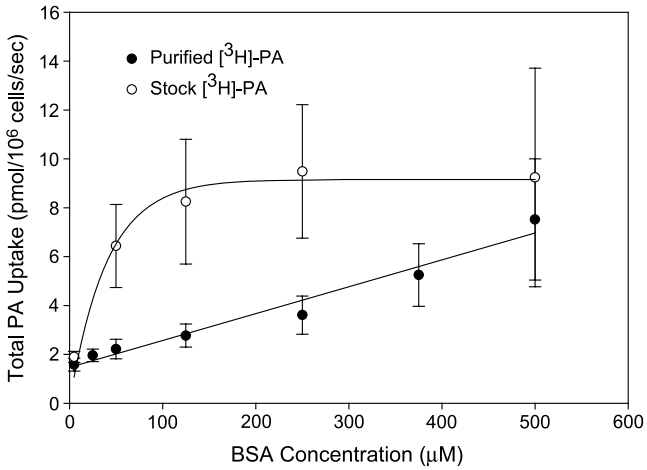

Fig. 3. PA uptake determined using both purified [^{3}H]PA and stock [^{3}H]PA *vs.* BSA concentration (5–500 μM) from isolated hepatocytes. In uptake studies using purified [^{3}H]PA, the unbound PA concentration remained constant at all BSA concentrations tested. Slope of the regression line was significantly different from zero (p < 0.0001) indicating that uptake was a nonsaturable increasing function of BSA concentration. Each data point represents mean ± SEM (n = 8). In experiments using stock [^{3}H]PA, the PA/BSA molar ratio was 0.3:1. Uptake in this case was a saturable function of increasing BSA concentration. Each data point represents the mean ± SEM (n = 5).

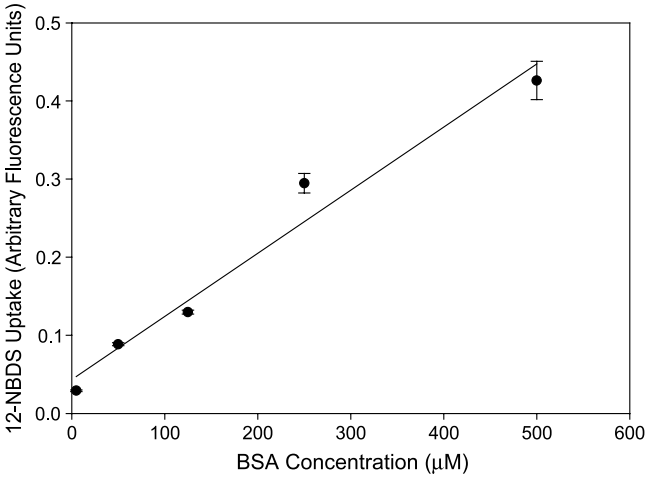

Fig. 4. Hepatocyte 12-NBDS uptake (arbitrary fluorescence units) *vs.* BSA concentration (5–500 μM) in the 1548 cell line. Molar ratios were adjusted to obtain similar unbound ligand concentration as [^{3}H]PA data. Slope of the regression line was significantly different from zero (p < 0.003) supporting the notion that uptake occurred from protein-bound and unbound fraction. Each data point represents mean ± SEM (n = 6).

beginning at about 250 μM BSA. However, slope of the apparent linear regression line (r = 0.97) was determined to be significantly different from zero (p < 0.003, n = 5).

Effect of L-FABP Antisera on [^{3}H]PA Clearance by 1548 Hepatoma Cells. To explore a possible role of a surface membrane transport protein-plasma binding protein interaction that might lead to a facilitated protein–ligand dissociation rate and hence enhanced uptake, purified [^{3}H]PA uptake studies were performed in the presence of L-FABP antisera, using 100 and 5 μM BSA (n = 6). Clearance of [^{3}H]PA in the presence of 100 μM (2.9 μL/s/

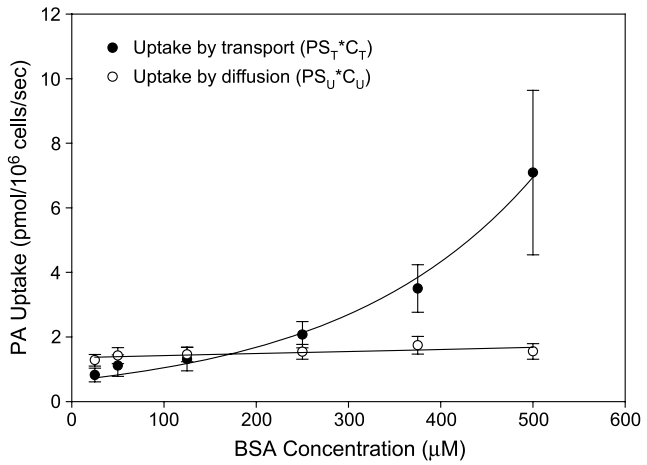

Fig. 5. Diffusive (PS_U*C_{Ux}) and transport (PS_T*C_{Tx}) components of PA uptake in isolated hepatocytes at different BSA concentrations (25–500 μM). Values were calculated for purified [^{3}H]palmitate uptake by hepatocyte suspension (Fig. 3) using Eqs. (10) and (11). The calculated PS_T*C_{Tx} values increased exponentially with increasing BSA concentration suggesting that the transport component is significantly increased with increasing protein concentration. The calculated PS_U*C_{Ux} values remained unchanged with increasing BSA concentration suggesting that the diffusive component was independent of extracellular albumin concentration.

Table I. Nonparametric Moments Analysis for Extracted [^{3}H]PA (Mean ± SD, n = 4)

Perfusate	E^a	MTT^b (s)	CV^{2c}
1% BSA	0.49 ± 0.14	17.48 ± 3.35	2.47 ± 0.89
1% BSA with L-FABP antisera	0.34 ± 0.07^d	24.81 ± 2.08^e	2.00 ± 0.72

[a] Hepatic extraction ratio (E) = 1 − hepatic availability (F).
[b] Mean transit time (corrected for the catheter transit time).
[c] Normalized variance.
[d] [^{3}H]PA has a significantly smaller E ($P < 0.05$) in 1% BSA perfusate with L-FABP antisera than that in 1% BSA perfusate without L-FABP antisera.
[e] [^{3}H]PA has a significantly longer MTT ($P < 0.05$) in 1% BSA perfusate with L-FABP antisera than that in 1% BSA perfusate without L-FABP antisera.

10^6 cells) and 5 μM (9.7 μL/s/10^6 cells) BSA was substantially reduced in the presence of L-FABP antisera by approximately 44 ± 4% (1.6 μL/s/10^6 cells) and 27 ± 2% (7.1 μL/s/10^6 cells) from the control values, respectively. The decrease in clearance was greater ($p < 0.01$) in the presence of the higher BSA concentration (100 μM) than in the lower BSA concentration (5 μM).

Permeability-Surface Area Products. Calculating the diffusive ($PS_U{*}C_{U100}$) and transport ($PS_T{*}C_{T100}$) components for [^{3}H]PA uptake studies (calculated using a tracer [^{3}H]PA concentration of 1 nM) at 100 μM BSA with the 1548 hepatoma cell line showed that the $PS_U{*}C_{U100}$ was 1.18 ± 0.03 fmol/s/10^6 cells, whereas $PS_T{*}C_{T100}$ was 2.03 ± 0.13 fmol/s/10^6 cells (n = 6). In the presence of antisera at 5 and 100 μM BSA, the calculated $PS_U{*}C_{U100}$ was not significantly different from the value in the absence of antisera (1.0 ± 0.4 fmol/s/10^6 cells) at the 100 μM BSA concentration, whereas $PS_T{*}C_{T100}$ was statistically lower at 0.59 ± 0.08 fmol/s/10^6 cells (n = 6). The results therefore suggest that the antisera did not affect the uptake of unbound [^{3}H]PA, but affected (reduced) uptake from the albumin-bound fraction, suggesting that the antisera selectively inactivated one or more plasma membrane fatty acid transporters.

Calculation of $PS_U{*}C_{Ux}$ and $PS_T{*}C_{Tx}$ at all BSA concentrations tested using isolated rat hepatocytes (using an unbound PA concentration that was adjusted to remain constant at each BSA concentration) showed that $PS_U{*}C_{Ux}$ was constant. The average $PS_U{*}C_{Ux}$ was calculated to be 1.5 ± 0.06 pmol/10^6 cells/s. $PS_T{*}C_{Tx}$, however, was nonlinearly related to BSA concentration (Fig. 5). Therefore, the assumption that PS products were albumin-independent was found to be true only with $PS_U{*}C_{Ux}$ but not with $PS_T{*}C_{Tx}$, suggesting that the transport component for uptake is albumin-dependent whereas the diffusive component is albumin-independent.

Uptake of [^{3}H]PA in Isolated Perfused Rat Livers. Table I lists the results of nonparametric moment analysis for [^{3}H]PA. The [^{3}H]PA hepatic extraction fraction was statistically smaller (34%) in the presence of 1% BSA perfusate containing antisera than that in the absence of antisera. [^{3}H]PA was also associated with a significantly longer mean transit time (MTT; $p < 0.05$) in 1% BSA containing L-FABP antisera. Kinetic parameters for [^{3}H]PA uptake are shown in Table II. [^{3}H]PA was associated with a statistically smaller k_1 (42%, $p < 0.05$), k_1/k_2 ratio ($p < 0.05$), and PS (42%, $p < 0.05$) values using 1% BSA perfusate with L-FABP antisera than that in 1% BSA perfusate without L-FABP antisera. In contrast, there were no significant difference in k_2, k_e, V_C, V_P, or CL_{int} values for [^{3}H]PA in the two perfusates. The addition of L-FABP antisera to uptake media did not affect the unbound fraction. These results indicated that L-FABP antisera inhibited a surface transport protein that mediated [^{3}H]PA uptake.

DISCUSSION

This work has shown that the uptake of [^{3}H]PA into the liver is dependent on both the passive and facilitated transport pathways. The resulting calculated permeability surface area product (PS) confirmed that both unbound and bound fractions of LCFA contributed to the flux, but only the PS for the protein bound fraction was reduced in the presence of L-FABP antisera. Hence, unbound PA is mainly taken up via the passive pathway, whereas protein bound PA is mainly taken up by facilitated pathways. The most likely facilitated pathways are hepatocellular membrane proteins with high affinity for fatty acids, e.g., fatty acid translocase (FAT/CD 36) or the membrane fatty acid-binding protein ($FABP_{pm}$) (16). The reduction in transport of the facilitated pathway by the L-FABP antisera of about 40% is consistent with the $FABP_{pm}$ pathway contributing about half of the total facilitated pathway.

Although great attention has been given to removing radiolabel impurities in obtaining the main results, uptake

Table II. Kinetic Parameters for Extracted [^{3}H]PA (Mean ± SD, n = 4)

Perfusate	k_1 (s^{-1})	k_2 (s^{-1})	k_e (s^{-1})	k_1/k_2	V_C (mL g^{-1} liver)	V_P (mL g^{-1} liver)	CL_{int} (mL min^{-1} g^{-1} liver)	PS (mL min^{-1} g^{-1} liver)
1% BSA	0.162 ± 0.013	0.015 ± 0.005	0.042 ± 0.026	11.76 ± 3.45	0.85 ± 0.08	0.32 ± 0.04	2.03 ± 1.06	83,984 ± 16,348
1% BSA with L-FABP antisera	0.094 ± 0.024^a	0.017 ± 0.004	0.034 ± 0.017	5.53 ± 1.06^b	0.79 ± 0.09	0.29 ± 0.05	1.84 ± 1.29	48,392 ± 7,514^c

k_1 = permeation rate constant, k_2 = efflux rate constant, k_e = elimination rate constant, V_C = water hepatocellular volume, V_P = volume of distribution of sucrose in the perfusate, Cl_{int} = intrinsic clearance, PS = permeability − surface area product.
[a] [^{3}H]PA was associated with a significantly smaller k_1 ($p < 0.05$) in 1% BSA perfusate containing L-FABP antisera than without the antisera.
[b] [^{3}H]PA was associated with a significantly smaller k_1/k_2 ratio ($p < 0.05$) in 1% BSA perfusate with L-FABP antisera than without the antisera.
[c] [^{3}H]PA has a significantly smaller PS ($P < 0.05$) in 1% BSA perfusate with L-FABP antisera than without the antisera. There is no significant difference in k_2, k_e, V_C, V_P, and CL_{int} values for [^{3}H]PA in the different perfusates.

results with the impure radiolabel may actually support the finding obtained with the pure compound. Impurities in the stock radiolabeled product seem to have faster uptake rates than the purified PA and by a process that is saturable. The radiolabeled impurities are present in higher concentrations (1–2%) compared to the much lower concentrations of unbound [^{3}H]PA (<0.1%). An apparent saturation of PA uptake is evident at about 100 μM BSA using stock solutions of [^{3}H]PA. The effectively zero PA uptake above 100 μM BSA for stock solution suggests negligible uptake by diffusion of free PA. The dominant role of membrane proteins, such as $FABP_{pm}$, in facilitating the uptake of PA is not surprising when it is recognized that unbound PA is both ionized and very surface-active at physiological pH and is, therefore, likely to be trapped at the first membrane site encountered. Additional support for the role of membrane fatty acid transporters is provided by work showing that clofibrate induction enhances intracellular fatty acid diffusion (21). Our own work, which suggests that PA uptake greatly differs between male, female, pregnant female, and clofibrate-treated rats (22), is also consistent with facilitated PA transport rather than unbound transport as the available evidence does not support a large variation in the sinusoidal surface area for each of these groups of animals.

Uptake of 12-NBDS is known to reflect the uptake process of other LCFA (40), and the issue of impurity does not arise with this substrate. Therefore, using similar adjusted molar ratios of stearate, we studied the uptake of 12-NBDS by 1548 hepatoma cells grown in monolayers. Use of 12-NBDS to study the hepatocellular fatty acid uptake is well established, showing similar binding characteristics to that of other LCFA (35,41–43) and is known to enter hepatocytes by the same uptake mechanism(s) as that of nascent stearate (44). Because the increase in intracellular fluorescence intensity over time reflected the amount of stearate taken up by cell monolayers (Fig. 4), qualitatively, these data were similar to those using purified [^{3}H]PA. The similarity in uptake profiles shows that any contribution by acidic radiolabeled impurities was probably negligible. The observation that 12-NBDS uptake increased with increasing BSA concentration was consistent with the observation made by Elsing *et al.* (35) using confocal laser scanning microscopy (CLSM). In their study, the absence of extracellular binding protein significantly reduced hepatocyte 12-NBDS uptake. Those observations provided evidence for the involvement of the extracellular binding protein in the overall hepatocyte LCFA extraction process. It seemed that the presence of albumin does facilitate the uptake of protein-bound ligands and that this process may be mediated by LCFA transport proteins within the plasma membrane (45).

We studied the involvement of plasma membrane transport proteins on the uptake process using L-FABP antibody in the extracellular uptake media. Such transporters include the liver plasma membrane fatty acid binding protein ($FABP_{pm}$), fatty acid receptor protein (FAR), fatty acid transport protein (FATP), and fatty acid translocase (FAT), which are believed to play an important role in the transmembrane translocation of LCFA (46,47). Membrane proteins such as $FABP_{pm}$ are thought to act as a translocase or flippase, transporting the fatty acid to the cytoplasmic leaflet of the membrane (48). Using liver plasma membrane vesicles, Stremmel *et al.* (49) reported that antibodies raised against $FABP_{pm}$ reduced oleate binding in the presence of albumin to isolated liver plasma membranes by 70%. Furthermore, uptake of oleate by isolated hepatocytes was inhibited by 65% when cells were incubated with the $FABP_{pm}$ antibody (50). It is also known that polyclonal antibody raised against L-FABP binds to $FABP_{pm}$ owing to their immunological similarities (31,49,51,52). Hence, we investigated the role of membrane transporters, such as $FABP_{pm}$, on the uptake of PA by perfusing livers with an antisera raised against rat cytosolic L-FABP followed by [^{3}H]PA uptake studies in isolated perfused livers and 1548 cell cultures.

Rabbit plasma containing L-FABP antisera was directly added to liver perfusates at a dilutional volume (perfusate/serum) of 700:1. Using this volume ratio, no apparent physiological effects were noted during the experimental time period—including the lack of substantial reduction in the unbound ligand fraction. The addition L-FABP antisera to the perfusate, however, resulted in a 31% decrease in the [^{3}H]PA extraction fraction (Table I). The reduction in extraction was likely due to an interaction between L-FABP antisera and a plasma membrane fatty acid transporter. Perfusion with the L-FABP antisera also resulted in a significant decline of the PA k_1/k_2 ratio by 47%. The reduced ratio reflected a decrease in k_1 rather than an increase in k_2 (see Table II). This is reasonable because for the antibody to affect k_2, it would have to traverse the plasma membrane and bind to L-FABP. It is likely that using a smaller dilutional volume (more antisera) would further decrease the extraction fraction. However, this may affect the BSA–PA binding characteristics.

The reduced clearance in the presence of L-FABP antisera was also observed in 1548 hepatoma monolayers. The reduced clearance was significantly greater ($p < 0.05$) at higher BSA concentrations (45 ± 4% with 100 μM) compared to lower BSA concentrations (27 ± 2% with 5 μM). We attribute this difference to reflect an increased interaction between BSA–PA and membrane transporter proteins. If the interaction was due to the unbound ligand being extracted by a transport protein, the percentage difference would be expected to be similar. However, because this difference was larger at the higher extracellular BSA concentration, this may reflect an interaction between extracellular BSA and the transport protein.

Although the antisera decreased clearance, the reduced value may reflect either a decrease in the uptake of the unbound ligand component (comprising both diffusion and transport) or a decrease in the interaction of the albumin-bound ligand-transport component of the uptake process. To distinguish between these two processes, we modeled the permeability-surface area product of the unbound and albumin-bound components according to Eqs. (10) and (11). Calculations showed that, although the diffusive component was not significantly affected by the antisera (1.18 ± 0.03 fmol/s/10^6 cells *vs.* 1.0 ± 0.4 fmol/s/10^6 cells, respectively), the transport component was significantly decreased by the presence of antisera (2.03 ± 0.13 fmol/s/10^6 cells ($n = 6$) *vs.* 0.59 ± 0.08 fmol/s/10^6 cells, respectively)—suggesting that transmembrane diffusion and interaction of the unbound ligand with the membrane-bound fatty acid transporters

remained unchanged in the presence of L-FABP antibody, whereas the interaction of the albumin-bound PA with the fatty acid transporter(s) was substantially reduced. The much higher reduction in uptake at 100 μM BSA suggested to us that at physiological concentrations the majority of uptake likely comes from the albumin-bound component. The greater $PS_U{*}C_U$ and $PS_T{*}C_T$ values obtained with isolated hepatocyte studies, which were conducted as cell suspensions rather than the hepatoma cells which were conducted as monolayers, may be attributed to two reasons. First, the BSA uptake solution used in isolated hepatocyte studies contained both tracer [^{3}H]PA and cold PA (added to adjust the molar ratio to obtain constant unbound PA concentrations), whereas the uptake solution in 1548 hepatoma uptake studies contained only tracer [^{3}H]PA. Second, the difference in absolute values may be due to the different cell types and different experimental conditions used such as differences in unstirred fluid layers (4,5,18). The increase in $PS_T{*}C_{Tx}$ with an increase in extracellular binding protein concentration, however, reflects the growing importance of uptake from the protein-bound fraction as the concentration of BSA increases.

The affinity of PA toward BSA ($K_d \sim 10^{-8}$ M) (25) is much greater than for $FABP_{pm}$ ($K_d \sim 10^{-7}$ M), which is greater than for cytosolic L-FABP ($K_d \sim 10^{-6}$ M) (51). An interaction between BSA and $FABP_{pm}$ (for example) could reduce the affinity of PA for the BSA binding site by inducing a conformational change in BSA, which facilitates ligand dissociation. The increased affinity for $FABP_{pm}$ at this time would provide a driving force for PA's transfer and binding to the membrane protein. A similar interaction at the inner membrane surface would explain the transfer to cytosolic L-FABP. Thus, the change in affinity induced by BSA–$FABP_{pm}$ or $FABP_{pm}$–L-FABP interactions would allow PA to flow down a gradient, whereby the cell is able to provide a chemical or protein binding driving force that moves LCFA from the extracellular side through to the cytosolic side of the cell membrane. The fact that uptake in the presence of the antisera was inhibited to a greater extent at higher extracellular BSA concentrations supports the notion of a protein–protein interaction. Whether this theory is attributable to other extracellular proteins is not known, but would seem to be likely. Such an interaction has been documented in other systems such as metabolite transfer via enzyme–enzyme complexes (53).

The present results also support the notion of an earlier work arguing that uptake occurs from both the unbound and protein-bound fractions and that extracellular albumin interacts with the plasma membrane to off-load the protein-bound ligand (5,9–11,13,14,54). Trigatti *et al.* reported a direct interaction of serum albumin with adipocytes that pointed to an involvement of albumin binding sites on the cell surface. They showed that oleate uptake by adipocytes significantly increased with an increase in albumin concentration when studies were conducted using the same protein/ligand molar ratio, suggesting that BSA somehow enhanced oleate uptake (7). Our group also reported a very good correlation between protein isoelectric point (pI) and hepatocyte uptake of [^{3}H]PA (12). Higher uptake rates were associated with proteins containing a net positive charge, suggesting an ionic interaction between extracellular proteins and the cell surface.

The significance of this work is evident when one applies the findings from the study to physiological conditions. If one assumes an ideal plasma albumin concentration of 4.6 g/100 mL, i.e., 650 μM albumin, then based on the present PS estimates, uptake of albumin bound PA by a facilitated process such as $FABP_{pm}$ would constitute 89% of the total uptake of PA. Even in severe liver disease where plasma albumin may have been reduced to 2.9 g/100 ml, i.e., 420 μM albumin, uptake of albumin bound PA by a facilitated process such as $FABP_{pm}$ would constitute 76% of the total uptake of PA. Hence, facilitated transport by binding proteins such as $FABP_{pm}$ dominate the overall uptake of LCFA by hepatocytes relative to the unbound fraction and uptake by a passive pathway. Under nonphysiological conditions, as commonly conducted in *in vitro* studies at low BSA concentrations, the amount of ligand that is protein-bound is also significantly reduced. In this case, the contribution to total uptake by the interaction between the protein–ligand complex and cell surface is expected to decrease.

In summary, results from our study lead us to accept the hypothesis that uptake of PA by hepatocytes occurs from both the albumin-bound and unbound fractions. The saturation kinetic profile reported previously using constant molar ratio studies was also observed in the present study; however, this was only observed with stock [^{3}H]PA. The enhanced uptake of LCFA uptake in the presence of extracellular proteins was observed using both [^{3}H]PA and the fluorescent substrate 12-NBDS. Thus, results cannot be attributed to radiolabeled impurities still present in our purified samples. Furthermore, studies conducted using antisera raised against L-FABP support the notion that an interaction between the BSA-bound ligand and cell surface leads to further ligand availability for the uptake process. A BSA–membrane protein interaction may explain the facilitation mechanism of hepatocellular ligand uptake.

ACKNOWLEDGMENTS

This work was supported by an operating grant from the Canadian Institute of Health Research Grant and National Health and Medical Research Council of Australia. G. Rajaraman gratefully acknowledges studentship support by a University of Manitoba Fellowship Award. Mr. GQ Wang is supported by a CIHR/Rx&D studentship.

REFERENCES

1. R. A. Weisiger and W. L. Ma. Uptake of oleate from albumin solutions by rat liver. Failure to detect catalysis of the dissociation of oleate from albumin by an albumin receptor. *J. Clin. Invest.* **79**:1070–1077 (1987).
2. A. B. Fleischer, W. O. Shurmantine, B. A. Luxon, and E. L. Forker. Palmitate uptake by hepatocyte monolayers. Effect of albumin binding. *J. Clin. Invest.* **77**:964–970 (1986).
3. P. D. Berk. How do long-chain free fatty acids cross cell membranes? *Proc. Soc. Exp. Biol. Med.* **212**:1–4 (1996).
4. F. J. Burczynski and B. A. Luxon. Is there facilitated uptake of fatty acids by the liver? Interpretation and analysis of experimental data. *Can. J. Physiol. Pharm.* **73**:409–420 (1995).
5. Z. S. Cai, F. J. Burczynski, B. A. Luxon, and E. L. Forker. On the design and interpretation of experiments to elucidate albumin-dependent hepatic uptake. *Am. J. Physiol.* **262**: G1127–G1137 (1992).

6. D. Zakim. Fatty acids enter cells by simple diffusion. *Proc. Soc. Exp. Biol. Med.* **212**:5–14 (1996).
7. B. L. Trigatti and G. E. Gerber. A direct role for serum albumin in the cellular uptake of long-chain fatty acids. *Biochem. J.* **308**:155–159 (1995).
8. K. J. Baker and S. E. Bradley. Binding of sulfobromophthalein (BSP) sodium by plasma albumin. Its role in hepatic BSP extraction. *J. Clin. Invest.* **45**:281–287 (1966).
9. E. L. Forker and B. A. Luxon. Albumin helps mediate removal of taurocholate by rat liver. *J. Clin. Invest.* **67**:1517–1522 (1981).
10. R. A. Weisiger, J. L. Gollan, and R. K. Ockner. The role of albumin in hepatic uptake processes. *Prog. Liver Dis.* **7**:71–85 (1982).
11. F. J. Burczynski, G. Q. Wang, B. Elmadhoun, Y. M. She, M. S. Roberts, and K. G. Standing. Hepatocyte [^{3}H]palmitate uptake: effect of albumin surface charge modification. *Can. J. Physiol. Pharm.* **79**:868–875 (2001).
12. B. M. Elmadhoun, G. Q. Wang, L. A. Kirshenbaum, and F. J. Burczynski. Palmitate uptake by neonatal rat myocytes and hepatocytes. Role of extracellular protein. *Eur. J. Biochem.* **268**:3145–3153 (2001).
13. F. J. Burczynski, G. Q. Wang, and M. Hnatowich. Effect of binding protein surface charge on palmitate uptake by hepatocyte suspensions. *Br. J. Pharmacol.* **120**:1215–1220 (1997).
14. E. L. Forker, B. A. Luxon, M. Snell, and W. O. Shurmantine. Effect of albumin binding on the hepatic transport of rose bengal: surface-mediated dissociation of limited capacity. *J. Pharmacol. Exp. Ther.* **223**:342–347 (1982).
15. W. Stremmel. Mechanism of hepatic fatty acid uptake. *J. Hepatol.* **9**:374–382 (1989).
16. W. Stremmel, L. Pohl, A. Ring, and T. Herrmann. A new concept of cellular uptake and intracellular trafficking of long-chain fatty acids. *Lipids* **36**:981–989 (2001).
17. L. H. Bernstein, J. B. Ezzer, L. Gartner, and I. M. Arias. Hepatic intracellular distribution of tritium-labeled unconjugated and conjugated bilirubin in normal and Gunn rats. *J. Clin. Invest.* **45**:1194–1201 (1966).
18. F. J. Burczynski, Z. S. Cai, J. B. Moran, and E. L. Forker. Palmitate uptake by cultured hepatocytes: albumin binding and stagnant layer phenomena. *Am. J. Physiol.* **257**:G584–G593 (1989).
19. B. A. Luxon. Inhibition of binding to fatty acid binding protein reduces the intracellular transport of fatty acids. *Am. J. Physiol.* **271**:G113–G120 (1996).
20. B. A. Luxon, M. T. Milliano, and R. A. Weisiger. Induction of hepatic cytosolic fatty acid binding protein with clofibrate accelerates both membrane and cytoplasmic transport of palmitate. *Biochim. Biophys. Acta* **1487**:309–318 (2000).
21. M. T. Milliano and B. A. Luxon. The peroxisomal proliferator clofibrate enhances the hepatic cytoplasmic movement of fatty acids in rats. *Hepatology* **33**:413–418 (2001).
22. D. Y. Hung, F. J. Burczynski, P. Chang, A. Lewis, P. P. Masci, G. A. Siebert, Y. G. Anissimov, and M. S. Roberts. Fatty acid binding protein is a major determinant of hepatic pharmacokinetics of palmitate and its metabolites. *Am. J. Physiol. Gastrointest. Liver Physiol.* **284**:G423–G433 (2003).
23. D. Y. Hung, G. A. Siebert, P. Chang, F. J. Burczynski, and M. S. Roberts. Reduced hepatic extraction of palmitate in steatosis correlated to lower level of liver fatty acid binding protein. *Am. J. Physiol. Gastrointest. Liver Physiol.* (2004).
24. F. C. Greenwood and W. M. Hunter. The preparation of ^{131}I-labelled human growth hormone of high specific radioactivity. *Biochem. J.* **89**:114–124 (1963).
25. B. M. Elmadhoun, G. Q. Wang, J. F. Templeton, and F. J. Burczynski. Binding of [^{3}H]palmitate to BSA. *Am. J. Physiol.* **275**:G638–G644 (1998).
26. B. Borgstrom. Investigation on lipid separation methods. Separation of cholesterol esters, glycerides and free fatty acids. *Acta. Physiol. Scand.* **25**:111–119 (1952).
27. F. J. Burczynski, S. M. Pond, C. K. Davis, L. P. Johnson, and R. A. Weisiger. Calibration of albumin-fatty acid binding constants measured by heptane–water partition. *Am. J. Physiol.* **265**:G555–G563 (1993).
28. A. A. Spector, J. E. Fletcher, and J. D. Ashbrook. Analysis of long-chain free fatty acid binding to bovine serum albumin by determination of stepwise equilibrium constants. *Biochemistry* **10**:3229–3232 (1971).
29. F. J. Burczynski, S. Fandrey, G. Wang, P. A. Pavletic, and Y. Gong. Cytosolic fatty acid binding protein enhances rat hepatocyte [^{3}H]palmitate uptake. *Can. J. Physiol. Pharm.* **77**:896–901 (1999).
30. W. Stremmel and P. D. Berk. Hepatocellular influx of [^{14}C]oleate reflects membrane transport rather than intracellular metabolism or binding. *Proc. Natl. Acad. Sci. USA* **83**:3086–3090 (1986).
31. W. Schwieterman, D. Sorrentino, B. J. Potter, J. Rand, C. L. Kiang, D. Stump, and P. D. Berk. Uptake of oleate by isolated rat adipocytes is mediated by a 40-kDa plasma membrane fatty acid binding protein closely related to that in liver and gut. *Proc. Natl. Acad. Sci. USA* **85**:359–363 (1988).
32. D. Sorrentino, R. B. Robinson, C. L. Kiang, and P. D. Berk. At physiologic albumin/oleate concentrations oleate uptake by isolated hepatocytes, cardiac myocytes, and adipocytes is a saturable function of the unbound oleate concentration. Uptake kinetics are consistent with the conventional theory. *J. Clin. Invest.* **84**:1325–1333 (1989).
33. S. M. Pond, C. K. Davis, M. A. Bogoyevitch, R. A. Gordon, R. A. Weisiger, and L. Bass. Uptake of palmitate by hepatocyte suspensions: facilitation by albumin? *Am. J. Physiol.* **262**:G883–G894 (1992).
34. J. Storch, C. Lechene, and A. M. Kleinfeld. Direct determination of free fatty acid transport across the adipocyte plasma membrane using quantitative fluorescence microscopy. *J. Biol. Chem.* **266**:13473–13476 (1991).
35. C. Elsing, U. Winn-Borner, and W. Stremmel. Confocal analysis of hepatocellular long-chain fatty acid uptake. *Am. J. Physiol.* **269**:G842–G851 (1995).
36. G. Wang, Q. M. Chen, G. Y. Minuk, Y. Gong, and F. J. Burczynski. Enhanced expression of cytosolic fatty acid binding protein and fatty acid uptake during liver regeneration in rats. *Mol. Cell. Biochem.* **262**:41–49 (2004).
37. K. Cheung, P. E. Hickman, J. M. Potter, N. I. Walker, M. Jericho, R. Haslam, and M. S. Roberts. An optimized model for rat liver perfusion studies. *J. Surg. Res.* **66**:81–89 (1996).
38. V. P. Dole. Fractionation of plasma nonesterified fatty acids. *Proc. Soc. Exp. Biol. Med.* **93**:532–533 (1956).
39. M. S. Roberts and Y. G. Anissimov. Modeling of hepatic elimination and organ distribution kinetics with the extended convection–dispersion model. *J. Pharmacokinet. Biopharm.* **27**:343–382 (1999).
40. B. A. Luxon and M. T. Milliano. Cytoplasmic codiffusion of fatty acids is not specific for fatty acid binding protein. *Am. J. Physiol.* **273**:C859–C867 (1997).
41. B. A. Luxon and R. A. Weisiger. Sex differences in intracellular fatty acid transport: role of cytoplasmic binding proteins. *Am. J. Physiol.* **265**:G831–G841 (1993).
42. E. J. Murphy. L-FABP and I-FABP expression increase NBD-stearate uptake and cytoplasmic diffusion in L cells. *Am. J. Physiol.* **275**:G244–G249 (1998).
43. J. Pohl, A. Ring, and W. Stremmel. Uptake of long-chain fatty acids in HepG2 cells involves caveolae: analysis of a novel pathway. *J. Lipid Res.* **43**:1390–1399 (2002).
44. J. G. Fitz, N. M. Bass, and R. A. Weisiger. Hepatic transport of a fluorescent stearate derivative: electrochemical driving forces in intact rat liver. *Am. J. Physiol.* **261**:G83–G91 (1991).
45. B. A. Fitscher, C. Elsing, H. D. Riedel, J. Gorski, and W. Stremmel. Protein-mediated facilitated uptake processes for fatty acids, bilirubin, and other amphipathic compounds. *Proc. Soc. Exp. Biol. Med.* **212**:15–23 (1996).
46. J. F. Glatz and G. J. van der Vusse. Cellular fatty acid-binding proteins: their function and physiological significance. *Prog. Lipid Res.* **35**:243–282 (1996).
47. J. F. Glatz, J. J. Luiken, and A. Bonen. Involvement of membrane-associated proteins in the acute regulation of cellular fatty acid uptake. *J. Mol. Neurosci.* **16**:123–132 (2001).
48. F. A. Van Nieuwenhoven, G. J. Van der Vusse, and J. F. Glatz. Membrane-associated and cytoplasmic fatty acid-binding proteins. *Lipids* **31**(Suppl):S223–S227 (1996).
49. W. Stremmel, G. Strohmeyer, F. Borchard, S. Kochwa, and P. D. Berk. Isolation and partial characterization of a fatty acid

binding protein in rat liver plasma membranes. *Proc. Natl. Acad. Sci. USA* **82**:4–8 (1985).
50. W. Stremmel and L. Theilmann. Selective inhibition of long-chain fatty acid uptake in short-term cultured rat hepatocytes by an antibody to the rat liver plasma membrane fatty acid-binding protein. *Biochim. Biophys. Acta* **877**:191–197 (1986).
51. R. J. Paulussen and J. H. Veerkamp. Intracellular fatty-acid-binding proteins. Characteristics and function. *Sub-cell. Biochem.* **16**:175–226 (1990).
52. W. Stremmel, G. Lotz, G. Strohmeyer, and P. D. Berk. Identification, isolation, and partial characterization of a fatty acid binding protein from rat jejunal microvillous membranes. *J. Clin. Invest.* **75**:1068–1076 (1985).
53. D. K. Srivastava and S. A. Bernhard. Metabolite transfer via enzyme–enzyme complexes. *Science* **234**:1081–1086 (1986).
54. F. J. Burczynski and Z. S. Cai. Palmitate uptake by hepatocyte suspensions: effect of albumin. *Am. J. Physiol.* **267**:G371–G379 (1994).